A98-31631 ICAS-98-5,3,2

OPTIMISATION OF A COMPOSITE BONDED REPAIR TO CRACKED PANELS SUBJECTED TO ACOUSTIC EXCITATION

R.J. Callinan[1], W.K. Chiu[2] and S.G. Galea[1]

[1]Airframes and Engines Division, Defence Science & Technology Organisation - Aeronautical & Maritime Research Laboratory, 506 Lorimer Street, Fishermens Bend, Victoria 3207, Australia.

[2] DSTO-Centre of Expertise in Structural Mechanics, Department of Mechanical Engineering, Monash University, Clayton, Victoria 3168, Australia.

Abstract

The skin of an aircraft can vibrate as a result of pressure waves caused by engine and/or aerodynamic effects. In modern fighter aircraft such as the F/A-18, sound pressure levels have been recorded up to 170 dB over the surface of the skin. In the F/A-18 cracking has occurred in the lower nacelle external skin, typically along the boundaries of the panel. These cracks often originate from a fastener line and grow along the boundary and then turn into the centre of the panel. In the case of the F/A-18, cracking was due to higher than expected pressure levels caused by an aerodynamic disturbance at the inlet lip. An attempt was made to repair a panel with a boron fibre patch however this repair did not appear to significantly reduce the crack growth. The design of the repair was based on in-plane loads only. This paper aims at developing a patch design, based on a finite element analysis, which significantly reduces crack stress intensity factor for structures subject to intense acoustic environments. A significant reduction in stress intensity is achieved by using a highly-damped patch which incorporates a uni-directional boron/epoxy repair surrounded by viscoelastic material, which provides the necessary damping, and [0/90] boron/epoxy constraining layers.

Introduction

Acoustic fatigue is due to a very high intensity excitation as a result of pressure waves caused by either engine or aerodynamic effects. Acoustically-induced cracking has occurred on the external surface of the lower nacelle skin on the F/A-18, as illustrated in Fig. 1. In these regions overall sound pressure levels greater than 170 dB have been measured in flight [(1)]. These high sound pressure levels appear to be a result of an aerodynamic disturbance at the inlet lip [(1)]. Typical cracks occur along a line of rivets or run parallel to the rivet line and may turn into the centre of the panel, as shown in the inset. Cracking generally occurs along the longer side of the panel where the bending stresses due to out-of-plane vibrations are a maximum. Up to a third of the F/A-18's in the RAAF fleet are affected by these cracks.

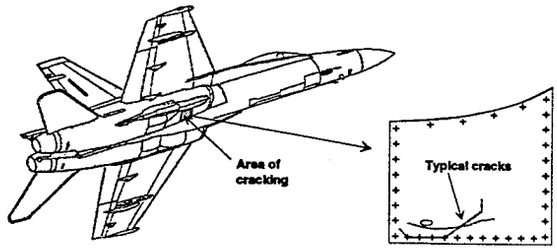

FIGURE 1 - Location of the cracking in the lower nacelle inlet.

The standard repair for such cracking is to remove and replace the panel. The standard long term fix is to incorporate additional stiffeners on the inside to stiffen the panel. This has two effects; firstly to reduce the panels response, i.e. lower stress for a given load and secondly it increases the resonant frequencies of the panel to frequencies well outside the recorded excitation frequencies.

In order to reduce the cost of repairing such cracked structures a bonded composite repair would be preferred. The benefits of such a repair are reflected in the time required to carry out the repair; typically 60 hours for the mechanical repair and approximately 15-25 hours for the bonded repair. Such a repair was designed, based on a standard repair design procedure, and implemented

on an existing cracked aircraft. While in the past boron fibre/epoxy resin patches have been extremely successful, in repairing cracked metallic secondary and primary structures[13], in this case significant crack growth occurred after the application of the repair. This unsuccessful application of a bonded repair to a cracked metallic structure was due to the fact that the standard design procedure[14] is based on in-plane static low cycle loading condition. However for the acoustic environment a new design approach for bonded repairs is required, i.e. a design procedure based on dynamic out-of-plane high-cycle loading. Work carried out by Callinan et al[2] showed that the addition of damping to a bonded repair can result in significant reductions of crack growth rate. These authors showed that a low-damping patch covering the entire panel resulted in a reduction of the mode *I* stress intensity, K_I, from 18 MPa $\sqrt{m}$, for a cracked unrepaired panel, to 6 MPa $\sqrt{m}$. Although this is not a high value in comparison with the fracture toughness value, K_{IC}, in an environment of high-cycle fatigue it leads to a high crack growth rate. They found that by further increasing the damping of the repaired structure, from a loss factor of 0.032 to 0.128, reduced the stress intensity to 4 MPa $\sqrt{m}$. Work carried out by Rodgers et al[3] and Liguour et al[4] also indicates that the addition of damping can significantly reduce the crack growth rate.

This paper reports on the design of a highly-damped bonded repair, incorporating constrained layered damping (CLD), using finite element analysis (FEA) of the structure subject to simulated acoustic loading conditions. The study involves the estimation of the root mean square (rms.) stress intensity factor (K) in the cracked and cracked/repaired cases. Various patch design parameters, such as reinforcing patch dimensions, thicknesses of the (viscoelastic) damping material and thickness of the constraining layer are considered in order to maximise the effectiveness of the patch and thus lower the stress intensity. Finally it is theoretically verified that the highly-damped patch can significantly reduce crack growth and therefore yield acceptable crack lengths for a 6000 hour lifetime condition.

Design of highly-damped patch

The work carried out by Rodgers et al[3] indicates that typical crack lengths are 100 mm long and occur in a skin thickness of approximately 1 mm. The repair must restore the stiffness of the structure, with an equivalent amount of composite material, and also reduce the dynamic stress levels using high damping viscoelastic materials (VEM).

Since the repairs are on the external surface there is a requirement to preserve aerodynamic smoothness. Therefore patch development is undertaken with the restriction that the patch must be tapered and the thickness must not exceed approximately 3 mm (1/8"). Rogers et al[3] considered this to be an adequate thickness since such an intrusion would not be significant with respect to the boundary layer on the aft 80% of any surface. Also the possible crack growth for a 6000 hour lifetime must be considered.

The process of designing a highly-damped patch is illustrated by the flow chart shown in Fig 2. The analysis begins with the definition of geometry, boundary conditions and appropriate material loss factors for the F.E. model of the cracked structure. The model is also subject to the input pressure PSD. Also incorporated within the model is the repair configuration to restore structural integrity. After the F.E. analysis is carried out, the rms stresses, strains, displacements and stress intensities must be considered. From crack growth data the likely crack size after 6000 hours can be estimated. If the crack growth exceeds the limit required at 6000 hours then a new (damping) material and geometric configurations must be considered. Clearly the damping material must be capable of achieving the assumed loss factor under the expected operating temperatures. That is, a reasonable estimate of the operating temperature is required since the material loss factor of the VEM is highly dependent on the operating temperature. Therefore accurate crack growth predictions will depend on accurate measurements of (i) load and strain levels, and resonant frequencies (needed to calibrate the F.E. model), (ii) operating temperature and VEM data and (iii) crack growth data (generated under high frequency bending conditions). The flow chart illustrates the systematic procedure used for changing the configuration until an acceptable design is achieved.

Damping of highly-damped patches

One of the most effective mechanisms to substantially reduce the dynamic stress level in the repaired structure is to increase the damping performance of the repair and, therefore, of the repaired structure. Callinan et al[2], Rogers et al[3]

and Liguour et al[4] reported on the use of a highly-damped composite patch (or 'Durability Patch') to prevent the further growth of costly 'nuisance' cracks. This is a passive damping technique aimed at reducing high-cycle fatigue. Rogers et al[3] noted that this type of application was rarely used for high-cycle fatigue because the necessary design information such as temperatures, resonant frequencies, and strain levels were difficult to obtain. They further reported that aircraft structures are often susceptible to resonant high-cycle fatigue due to the low intrinsic damping of the material since rms stress levels are highly dependant on modal damping. Thus in order to increase damping the authors considered the use of constrained layer damping which increases the structural damping of the repaired structure and will assist in stopping or substantially reducing acoustically-induced crack growth in the panel. There are numerous case studies, noted by Soovere & Drake[5], of the use of damping in the aeronautical scene to alleviate problems associated with resonant vibrations. In this section the modal loss factor of a reinforced panel is calculated for various bonded doubler reinforcement geometries, add-on damping treatment geometries and constraining layer effective stiffnesses. This damping study is undertaken on a panel similar to that shown in Fig. 3 except that no crack is included and the reinforcement now has its centreline (i.e. the centre of the W dimension) aligned with the centreline of the long dimension of the panel.

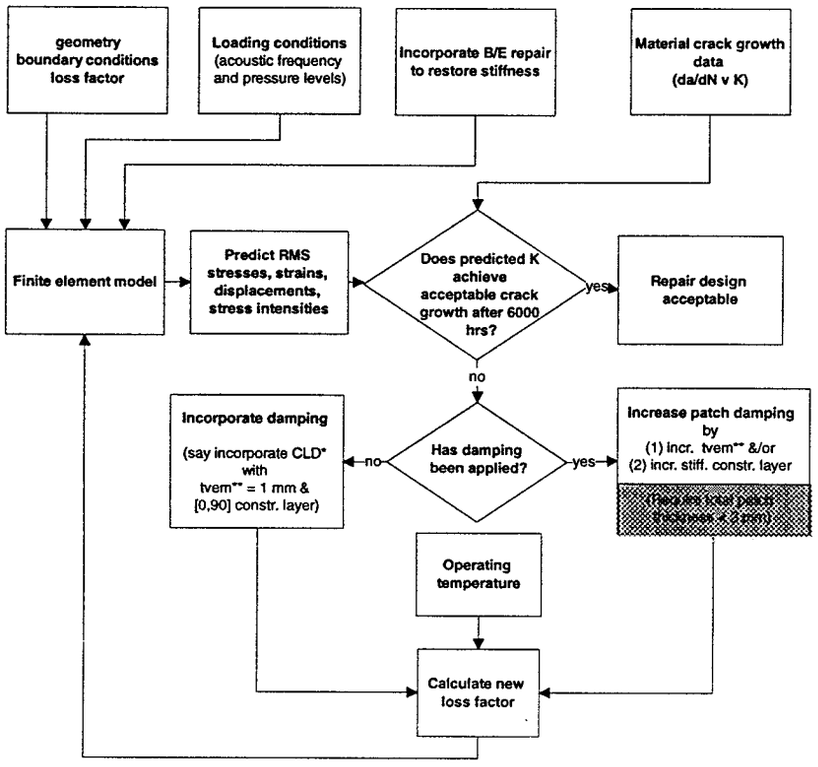

FIGURE 2 - Flow chart for designing highly-damped repairs for acoustically-induced cracked skins.

Initially an investigation into the effect of reinforcement geometry on modal loss factor is undertaken. In this case a 250 mm long by 166 mm wide by 1.2 mm thick aluminium panel, fixed on all four sides, is modelled. The entire aluminium panel is treated with a layer of constrained layer damping. Typical 'off-the-shelf' constrained layer damping treatments are 0.5 to 2 mm thick with a 0.125 mm thick constraining layer of aluminium. Material properties for the damping (VEM) material, aluminium and boron/epoxy are given in Table 1. The material loss factor for the viscoelastic material is taken as 1.0 and the constraining layer is an aluminium sheet 0.125 mm

thick. The panel is reinforced with a unidirectional boron/epoxy laminate with fibres aligned in the y-direction, see Fig. 3. The thickness of this reinforcement is determined such that the stiffness of the reinforcement and the aluminium plate are matched, i.e. using equation (1)

$$E_{al}\, t_{al} = E_r\, t_r \qquad (1)$$

These studies were conducted with a reinforcement of constant length (L) of 75 mm and varying widths (W) of 50 mm, 100 mm and 125 mm. The effects of these different size reinforcements on the structural loss factor of the panel are determined and are given in Table 2. It must be pointed out at this stage that the damping properties of the boron/epoxy laminate are not included in the analysis. Therefore, the actual structural damping is expected to be higher than that predicted in this study, hence, the results from this study are conservative. The modal loss factor is calculated from the finite element analysis by assuming that, given the material damping, the modal structural loss factor can be calculated by:

$$\eta_s = \Sigma_{i=1 \text{ to } n}\, \eta_i\, e_i / e \qquad (2)$$

where η_s is the structural loss factor and η_i is the material loss factor of the i th element. The modal energy, e, is calculated with equation (3);

$$e = \int \delta^T [K]\, \delta\, dV \qquad (3)$$

Where δ is the eigenvector and the stiffness matrix is denoted by [K]. Equation (2) is implemented as a post-processing option in our finite element analysis package and was first validated prior to its use.

The results in Table 2 show that the size of the unidirectional boron/epoxy reinforcement has a small effect on the structural damping. However, Chiu et al[6] observed that when the reinforcement was made from aluminium changing the size of the reinforcement caused a large change in the modal loss factor. For example, when the size of the boron/epoxy reinforcement is increased from 75 mm by 50 mm to 75 mm by 125 mm, there is only a 5 % reduction in the modal loss factor for mode 1 compared to an 11 % reduction for the aluminium reinforcement.

Table 3 shows the results for modal loss factors when only the boron/epoxy patch is treated with constrained layer damping. This table shows that the structural damping derived with this scheme of damping treatment is not very effective. These results therefore confirm that damping treatment should be applied to the entire panel for more effective damping of the structure.

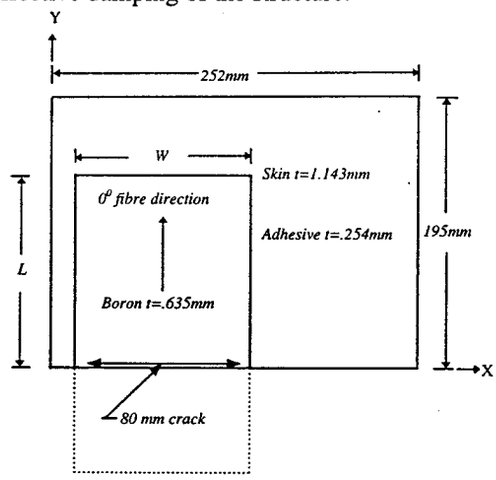

FIGURE 3 - Dimensions of simplified F/A-18 nacelle inlet panel, with crack and boron/epoxy patch.

The investigation is extended to a panel with dimensions shown in Fig. 3 without the crack and with the reinforcement centred as described above. In this analysis only one patch size is considered, viz. 77 mm long by 125 mm wide, but the VEM thickness, t_{VEM}, is varied from 0.5 mm to 2.0 mm. The constraining layer is now boron/epoxy and two laminates are modelled, viz. a 2 ply [0/90] laminate and a 4 ply $[0/90]_{sym}$ laminate.

Material	Young's modulus (MPa)	Poisson's ratio	Shear modulus (MPa)	Density ($x10^{-9}$ Mg/mm^3)
Aluminium	71000.	0.33	26691.	2.77
Adhesive	2273	0.35	842.	1.2
Boron	207000.	0.21	4800.	2.0
VEM (20°C)	5700	0.30		1.75

TABLE 1- Material properties used in the FEA.

Mode	Damped natural frequency (Hz)	Loss factor	Specimen description
1	290	0.139	Patch dimensions are
2	460	0.113	75 mm (L) x 50 mm (W)
3	769	0.081	
1	288	0.135	Patch dimensions are
2	441	0.118	75 mm (L) x 100 mm (W)
3	723	0.093	
1	289	0.132	Patch dimensions are
2	442	0.116	75 mm (L) x 125 mm (W)
3	732	0.085	

TABLE 2 - Loss factor of aluminium panel (with no crack) reinforced with unidirectional boron/epoxy with a 1 mm thick damping treatment and 0.125 mm thick aluminium constraining layer applied to whole panel.

Mode	Damped natural frequency (Hz)	Loss factor	Specimen description
1	324	0.03	Patch dimensions are
2	543	0.011	75 mm (L) x 50 mm (W)
3	852	0.022	
1	316	0.049	Patch dimensions are
2	501	0.03	75 mm (L) x 100 mm (W)
3	833	0.036	
1	315	0.053	Patch dimensions are
2	492	0.036	75 mm (L) x 125 mm (W)
3	830	0.036	

TABLE 3 - Loss factor of aluminium panel (with no crack) reinforced with unidirectional boron/epoxy with a 1 mm thick damping treatment and 0.125 mm thick aluminium constraining layer applied to the reinforcement only.

Mode	Damped natural frequency (Hz)	Loss factor	Specimen description
1	258	0.122	
2	449	0.106	t_{vem} = 0.5mm
3	641	0.078	[0/90] boron/epoxy constraining layer
1	240	0.161	
2	411	0.132	t_{vem} = 1.0 mm
3	597	0.091	[0/90] boron/epoxy constraining layer
1	217	0.232	
2	368	0.178	t_{vem} = 2.0 mm
3	528	0.126	[0/90] boron/epoxy constraining layer
1	245	0.216	
2	423	0.163	t_{vem} = 1 mm
3	585	0.122	$[0/90_{sym}]$ boron/epoxy constraining layer
1	222	0.274	
2	378	0.203	t_{vem} = 2 mm
3	528	0.1	$[0/90_{sym}]$ boron/epoxy constraining layer

TABLE 4 - Loss factor of aluminium panel (with no crack) reinforced with a unidirectional boron/epoxy patch of dimensions 77 mm (L) x 125 mm (W) with the constrained layer damping treatment applied to whole panel.

The predicted results are given in Table 4. Table 4 shows a significant increase in modal loss factor as the VEM thickness is increased. For mode 1 an increase of 32 % and 90 % is observed when the VEM thickness is increased from 0.5 mm to 1.0 mm and 0.5 mm to 2 mm, respectively. With the increase in thickness of the VEM there is also a corresponding drop in damped natural frequency which is mainly due to the increase in mass. Also increasing the effective stiffness of the constraining layer substantially improved the modal loss factor of the panel. For the 1.0 mm thick VEM case the loss factor, for the first resonant mode, increased by 34 % when the effective stiffness of constraining layer is increased by substituting the [0/90] laminate with a $[0/90]_{sym}$ laminate. The increase in loss factor is less pronounced for the 2.0 mm thick VEM case where an increase in 18% was observed when the constraining layer thickness is increased from 2 to 4 plies.

Overall this theoretical study has shown that the modal loss factor of the reinforced panel can be significantly improved by incorporating constrained layered damping. Further improvements can be achieved by increasing (i) the thickness of the VEM and (ii) the effective stiffness of the constraining layer. The values of modal loss factor of panels incorporating highly-damped patches, tabulated in Table 4, are used in the next section as inputs for the FE models of repaired cracked panels.

Analysis of unrepaired cracked and repaired cracked panels

Random response analysis

The random response analysis capability of the NASTRAN program has been used to solve this problem[7]. This involves a solution in the frequency domain after the transfer function, $H(\omega)$, is generated. Together with the power spectral density (PSD) of the excitation, $S_I(\omega)$, the PSD of the response, $S_J(\omega)$, is determined:

$$S_J(\omega) = |H(\omega)|^2 S_I(\omega) \qquad (4)$$

This analysis allows the statistical properties of the system to be evaluated. Random vibrations considered here involve all frequencies at any one instant in time. After calculating the PSD, the root mean square (rms) of the response can be determined by computing the square root of the PSD area:

$$j_{rms} = \sqrt{\frac{1}{2\pi}\int_0^\infty S_j(\omega)\, d\omega} \qquad (5)$$

A similar application of finite element techniques to undertake a PSD analysis to acoustic fatigue problems has been reviewed by Climent and Casalengua[8].

Stress intensity factors

In the F.E. model the depth of the plate is modelled using a single layer of 20 noded brick elements and as such, will model bending behaviour of the skin. The skin thickness is approximately 1 mm, hence the condition of plane stress is assumed. The computation of the stress intensity factor may be determined directly from the crack tip element used around the crack tip or from displacements using a crack opening (COD) formula. The rms crack tip stress intensity factors for mode *I II* and *III* are derived from the standard asymptotic relations:

$$K_{I\,rms} = \frac{E\,U_{rms}}{4}\sqrt{\frac{2\pi}{l}} \qquad (6)$$

$$K_{II\,rms} = \frac{E V_{rms}}{4}\sqrt{\frac{2\pi}{l}} \qquad (7)$$

$$K_{III\,rms} = G W_{rms}\sqrt{\frac{2\pi}{l}} \qquad (8)$$

where

E = Young's modulus,

G = Shear modulus

U_{rms} = mode *I* crack opening rms displacement (i.e. displacement out of plane of crack)

V_{rms} = mode *II* crack opening rms displacement (i.e. displacement in-plane, parallel to plane of crack)

W_{rms} = mode *III* crack opening rms displacement (i.e. displacement in-plane, transverse to plane of crack)

l = length of the crack tip element

The complexity of the random response analysis and number of assumptions made was such that validation of the analysis was necessary. The methodology was validated by comparing finite element results with experimental data published in (9) for a clamped plate with increasing crack length. The results are in reference (2) and show that the F.E. results are within 10% of the experimental results.

Analysis of unrepaired cracked plate

Previous work in (2) has established the stress intensity in the cracked (unrepaired) plate as shown in Fig. 4. The right hand crack tip refers to the crack tip located midway along the plate shown in Fig. 3. The higher stress intensity for the right hand crack tip is due to the larger dynamic bending stresses that occur midway along the panel. For a crack length of 80 mm K_I =15 MPa $\sqrt{m}$. Although this is not a high value in comparison with the fracture toughness value, K_{IC}, in an environment of high-cycle fatigue it leads to a high crack growth rate.

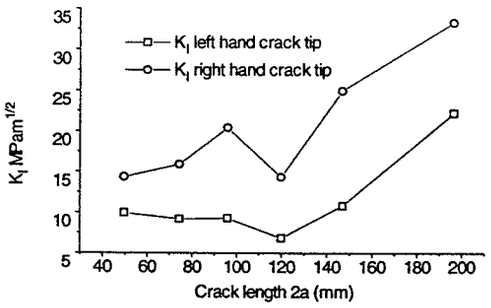

FIGURE 4 - Variation of mode I stress intensity as a function of crack length, ref (2).

Analysis of repaired cracked plate

Firstly, the panel is idealised as a three dimensional flat plate using 20 noded brick elements. Sufficient elements are used to define the crack length considered. The main reason that 20 noded bricks are used in the skin is that calculations for K can be made corresponding to a bending field. Also, the behaviour of the adhesive and viscoelastic damping materials is modelled as a 3 dimensional element, to allow for shear deformation. The boron/epoxy patch and boron/epoxy constraining layer are sufficiently thin such that 2D shell elements are an adequate representation.

The geometry of the structure is shown in Fig. 3. The mesh size of the skin and viscoelastic structure is 75x60 elements. As shown, the unidirectional boron/epoxy reinforcing patch only extends partially across the panel. It also covers an adjacent panel as shown in the dotted outline. The boron/epoxy repair has length, L, and width, W. In this section the length is fixed at 77 mm, however three widths are considered, viz. 80 mm, 99 mm and 126 mm. The entire panel is covered with the CLD material. Material properties for the skin, adhesive, damping material and boron are shown in Table 1.

The boundary conditions for this model are considered to be fully clamped except for the crack region which is not restrained. The patch above the crack also remains fully constrained. Clearly crack closure will occur at an increasing distance away from the crack tip, however the complexity in introducing such constraints is not included in this preliminary study.

Results and Discussion

Mode	Resonant frequency (Hz)
1	218
2	374
3	506

TABLE 5 - Frequencies for original uncracked unrepaired plate.

	Case 1.0/80*	Case 1.0/126*	Case 2.0/80*	Case 2.0/126*
Mode	Resonant frequency (Hz)			
1	208	216	193	200
2	335	341	308	319
3	442	461	403	417

TABLE 6 - Resonant frequencies for various patch widths (W) and thicknesses of damping material with [0/90] boron/epoxy constraining layer. (* a/b refers to values of t_{VEM}/W in mm.)

Modal shapes and frequencies. As previously mentioned, one of the main concerns regarding a particular repair is the change of frequency of the plate to those recorded excitation frequencies. The first three frequencies of the original uncracked unrepaired plate are shown in Table 5. For a highly-damped patch consisting of a 1.0 mm thick damping layer with a [0/90] boron/epoxy constraining layer the variation of resonant frequencies with increasing patch width (W) is shown in Table 6. The reinforcing patch length (L) is 77 mm. In all cases the addition of the highly-damped patch configuration resulted in a reduction of frequency. The resonant frequency increases by 5 %, 10 % and 13 % for vibration modes 1, 2 and 3, respectively, when the patch width increased from 80 to 126 mm. The first three modes are shown in Figs. 5, 6 and 7. The resonant frequencies for a 2.0 mm thick damping layer with a [0/90]

boron/epoxy constraining layer for various patch widths (W) are shown in Table 6.

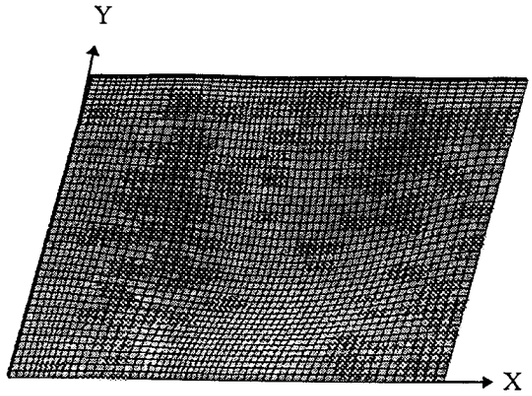

FIGURE 5 - Mode shape for mode 1 (211 Hz).

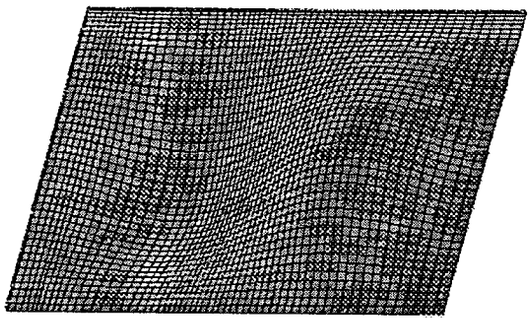

FIGURE 6 - Mode shape for mode 2 (335 Hz).

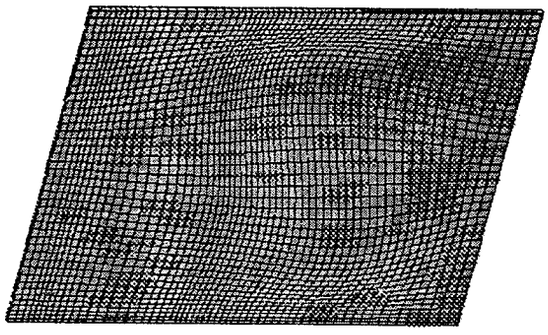

FIGURE 7 - Mode shape for mode3 (458 Hz).

PSD of the displacement. Since the area under the displacement PSD curve is the mean square displacement response, then a running integral of the displacement PSD illustrates the contribution of each vibration mode to the overall displacement response, as shown in Fig. 8. Since the stress intensity is proportional to the crack opening displacement, then a running integral of the displacement response will indicate the contribution of each vibration mode to the overall stress intensity. Fig. 8 shows the PSD displacement response at the right hand (inner side) crack for the case of a 1.0 mm thick damping layer with [0/90] boron/epoxy constraining layer and a 80 mm wide by 77 mm long boron/epoxy patch. Fig. 8 shows that vibration mode 1 contributes up to 99% of the overall stress intensity.

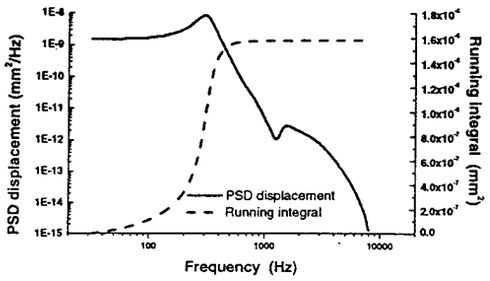

FIGURE 8 - PSD of displacement (αK_I) and running integral of the PSD for a panel with a 1.0 mm thick damping layer with [0/90] boron/epoxy constraining layer and an 80 mm wide by 77 mm long boron/epoxy reinforcement.

Stress intensity factor. Stress intensity factors are computed at the inside and outer surfaces of the skin. Since the repair results in a neutral axis shift the maximum values exist at the inner surface. The most critical crack tip position is the tip located midway down the longest side of the panel, as shown in Fig. 3. The maximum values have been plotted in Figs. 9, 10, 11 and 12. Various highly-damped patch configurations, involving 0.5, 1.0 and 2.0 mm thick damping VEM, are considered. In all cases the highly-damped patch has a boron/epoxy reinforcement/repair with dimensions 77 mm long and varying widths of 80 mm, 99 mm and 126 mm. Over the range of damping thickness considered the configuration that give the lowest values of K_I is for the 77 mm long by 126 mm wide reinforcement/repair with the 1.0 mm thick VEM and [0/90] constraining layer case. Also, the 0.5 mm thick VEM with [0/90] constraining layer case gave similar stress intensities as shown in Fig. 10.

Although no crack growth data corresponding to K_{II} or K_{III} stress intensities are available, the numerical values of K_{II} are lower than those for K_I, as shown in Fig. 11. Also, the numerical values for K_{III}, as shown in Fig. 12, are numerically comparable to K_I. All of the damped repairs are equally effective in reducing K_{II}, and show a considerable reduction in comparison to the low damped design. Also the results for K_{III} show that all the configurations, except the 0.5 mm, [0/90]

configuration, gave equally low values of K_{III}. Overall, comparisons with the low damped patch, i.e. a repair with no CLD included, have shown the highly-damped patch to be very effective. The best overall results appear to be for the 1.0 mm [0,90] configuration.

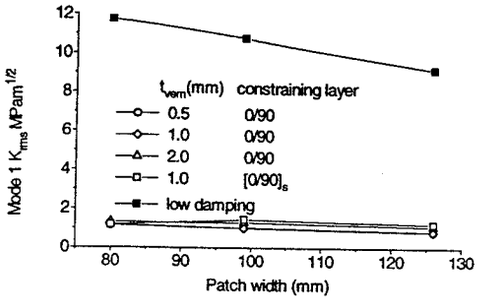

FIGURE 9 - Mode *I* stress intensity factor for various highly-damped and low damped patch configurations.

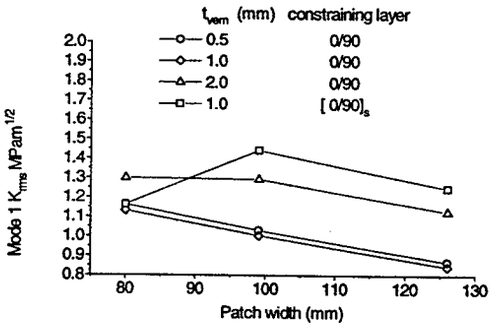

FIGURE 10 - Mode *I* stress intensity factor for various highly-damped patch configurations.

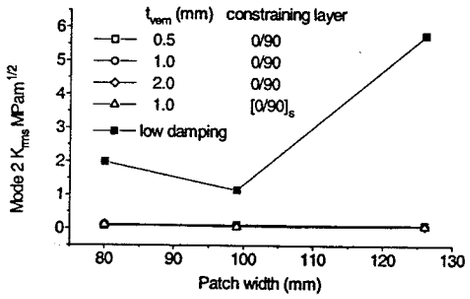

FIGURE 11 - Mode *II* stress intensity factor for various highly-damped and low damped patch configurations.

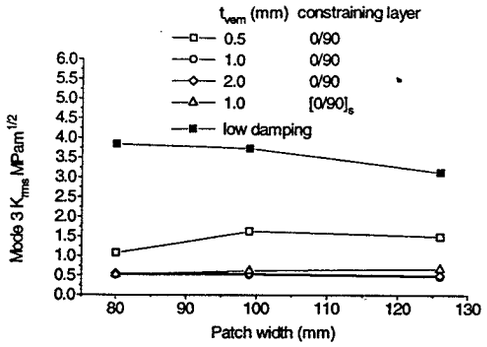

FIGURE 12 - Mode *III* stress intensity factor for various highly-damped and low damped patch configurations.

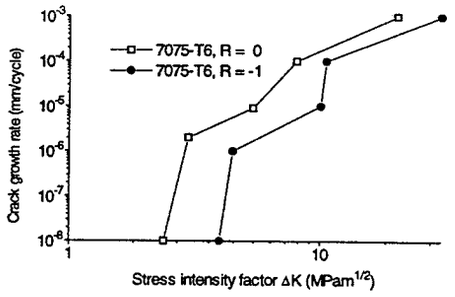

FIGURE 13 - Crack growth rate for 7075-T6 with increasing K_I (ref (10)).

Crack growth predictions. The crack growth data shown in Fig. 13 is for 7075-T6 corresponding to long crack growth data for panels tested in tension[10]. As a result of the neutral axis offset the curve of $R = 0$ most closely represents the crack growth curve. While these data are for low frequency loading conditions, evidence exists that high frequency testing results in slightly lower crack growth rates[11,12]. In our case high frequency bending is involved, therefore taking crack growth rates from Fig. 13 will lead to conservative estimates of crack length. The curve in Fig. 13 has been extrapolated to determine the approximate crack growth rate for cases less than 10^{-8} mm/cycle. Using these data insignificant crack growth has been calculated, after the 6000 hrs, for all the highly-damped patch configurations considered. Crack growth data for 4% Cu-Al alloy subjected to high frequency bending, given in reference (12), also indicates negligible crack growth for all the highly-damped patch configurations considered. Although no crack

growth data corresponding to K_{II} or K_{III} stress intensities are available the K_{III} results shown in Fig. 12 indicate possible crack growth for the 0.5 mm [0,90] configuration. Note that the above results are highly dependent on the material loss factors used in the modelling. This loss factor is also dependent on the operating temperature.

Conclusions

A methodology is proposed to enable the design highly-damped patches for cracked structures subject to intense acoustic loading. The highly-damped patch incorporates a boron/epoxy reinforcement/repair, to restore structural strength, as well as a constrained layered damping layer in order to enhance damping and thus reduce dynamic stresses. The proposed highly-damped patches reduce the resonant frequencies of the patched panel compared to the unrepaired uncracked panel. A study investigating the effects of various reinforcement dimensions, VEM thicknesses and constraining layer configurations on the modal loss factor of the plate is also undertaken. It is found that for the various reinforcements studied, no significant variation in loss factor was observed. However significant increases in loss factor are observed with increasing VEM thickness and constraining layer effective stiffness.

The inclusion of damping in the repair enables the stress intensity factor to be substantially reduced. Predictions of K_I indicates that no crack growth is expected for all the highly-damped patched configurations considered.

Acknowledgments

The authors would like to acknowledge Mr. Steve Sanderson for assistance in the finite element analysis.

References

(1) A/B/C/D Aircraft Lower Nacelle Skin Acoustic and Strain Measurements and Sonic Fatigue Analysis. MDC 94B0044. Mar, 1994.

(2) R.J. Callinan, S.C. Galea and S. Sanderson. Finite element analysis of bonded repairs to edge cracks in panels subjected to acoustic excitation. Composite Structures vol. 38, no. 1-4, p. 649-600, 1997.

(3) L. Rogers, J. Maly, I.R. Searle, R.I. Begami, W. Owen, D. Smith, R.W. Gordon, D. Conley 1997(b) Durability patch: Repair and life extension of high-cycle fatigue damage on secondary structure of ageing aircraft, 1st Joint DoD/FAA/NASA Conference on Aging Aircraft, Ogden, Ut, 8-10 July 1997.

(4) S. Liguour, R. Perez, K. Walters, 1997 Damped composite bonded repairs for acoustic fatigue, AIAA Paper 97-1689(A97-26775) AIAA/CGAS Aeronautics Conference, 3rd, Altanta, GA, May 12-14 1997, pp 774-783.

(5) J. Soovere and M.L. Drake "Aerospace structures technology damping design guide – Volume II: Design Guide, AFWAL-TR-84-3089, 1985.

(6) W.K. Chiu, S.C. Galea and R.J. Callinan. Damping of repaired structures subject to acoustic fatigue. To be submitted to Polymers and Polymer Composites.

(7) Blakely MSC/NASTRAN, basic dynamics analysis, user's guide. The MacNeal-Schwendler Corporation, Dec,1993.

(8) H. Climent and J. Casalengua. Application of a PSD technique to acoustic fatigue Stress Calculations in Complex Structures. Symposium on ' Impact of Acoustic Loads on Aircraft Structures', Lillehammer, Norway, May 1994.

(9) K.P. Byrne, Strains Affecting the Growth Rate of Edge Cracks in Acoustically Excited Panels. ISVR Tech. Rep. 59, Nov, 1972.

(10) J.C. Newman and P.R. Edwards. Short-Crack Growth Behaviour in Various Aircraft Materials. AGARD-12-767.

(11) A. Hartman, F.A. Jacobs, A. Nederven and P. de Rijk, Frequency Effect on 1mm 7075-T6 Clad Sheet. NLR TR M 2182, May 1967.

(12) K.P. Byrne, Bending-Induced Crack Propagation in a 4% Cu-Al Alloy with Reference to Acoustically Propagated Fatigue Cracks. Journal of Sound and Vibration, Vol 42, No 3, p. 337 - 355, 1975.

(13) A. A Baker, "Bonded Composite Repair of Metallic Aircraft Components", AGARD-CP-550 Composite Repair of Military Aircraft Structures, Paper 1, 1994.

(14) Composite Materials and Adhesive Bonded Repairs. RAAF Standard Engineering C5033, Draft - January 1994.